Proactive Control for Online Individual User Adaptation in a Welfare Robot Guidance Scenario: Toward Supporting Elderly People

Alejandro Pequeño-Zurro†, Jevgeni Ignasov†, Eduardo R. Ramírez, Frederik Haarslev, William K. Juel, Leon Bodenhagen, Norbert Krüger, Danish Shaikh, Iñaki Rañó *Member, IEEE*, and Poramate Manoonpong*, *Senior Member, IEEE*

***Abstract*—Due to demographic change, health and elderly care systems are facing a shortage of qualified caregivers. This issue can be addressed by introducing welfare robots into people's homes, hospitals, and care institutions. To provide useful support, such robots must adapt to individual users and smoothly interact with them. From this perspective, we present advances on the development of proactive control for online individual user adaptation in a welfare robot guidance scenario, with the integration of three main modules: navigation control, visual human detection, and temporal error correlation-based neural learning. The proposed control approach can drive a mobile robot to autonomously navigate in relevant indoor environments. At the same time, it can predict human walking speed based on visual information without prior knowledge of personality and preferences (i.e., walking speed). The robot then uses this prediction to continuously adapt its speed to individual users in a proactive online manner. We validate the performance of the proposed proactive robot control in different real-world environments with various users, including an elderly resident of a Danish elderly care center. The results show that the robot successfully and smoothly guided various users of different ages and average walking speeds (e.g., 0.2 m/s, 0.7 m/s, 1.1 m/s) to target locations over distances of 25-60 m. All in all, this study captures a wide range of research from robot control technology development to technological validity in a relevant environment and system prototype demonstration in an operational environment (i.e., an elderly care center).**

***Index Terms*—Service mobile robot, Neural control, Adaptive behavior, Welfare robot, Guide robot, Social robot, Human-robot interaction.**

I. Introduction

Demographic change constitutes a key challenge for health and elderly care systems in many societies since forecasts show that the population aged above 64 will grow by more than 70% in most countries [1]. A shortage of qualified caregivers is becoming a pressing issue in care facilities, and this deficit is expected to increase further with the imminent demographic shift. Welfare robots providing services in the health and elderly care sector are expected to be able to alleviate this shortage. They can help staff in their daily work while allowing the elderly with physical or mental conditions to remain independent for longer.

Fig. 1. Example of the SMOOTH robot with proactive control for online individual user adaptation in a guidance scenario. The robot navigates and guides the user in the relevant environment (e.g., inside a build at the University of Southern Denmark (SDU)). The proactive robot system has been successfully demonstrated to support elderly people in an operational environment (i.e., the Ølby elderly care center in Køge, Denmark).

Our recent SMOOTH project[1] deals with the problem of developing proactive and responsive robot behavior control to achieve smooth and fluent human-robot interaction in elderly care centers/nursing homes. We have identified elements of its main functionality to enable the robot to provide support to end-users (caregivers and elderly people) in elderly care institutions, leading to three key use cases. The use cases entail guiding the elderly to different areas of the elderly care facility (use case 1, see Fig. 1 for the simulated use case), transporting laundry and garbage (use case 2), and serving beverages to increase the liquid intake of the elderly (use case 3). Some of these use cases involve elements of individual

A. Pequeño-Zurro, J. Ignasov, D. Shaikh, and I. Rañó are with the Embodied Artificial Intelligence and Neurorobotics Laboratory, SDU-Biorobotics section, The Mærsk Mc-Kinney Møller Institute, The University of Southern Denmark, Odense 5230, Denmark, e-mail: (alz, igje, igra, danish)@mmmi.sdu.dk. A. Pequeño-Zurro is also with Laboratory of Neural Computation, Istituto Italiano di Tecnologia, Via Enrico Melen 83, Genova, Italy. †These authors contributed equally to this work.

E.R. Ramírez, F. Haarslev, W.K. Juel, L. Bodenhagen, and N. Krüger are with SDU-Robotics section, The Mærsk Mc-Kinney Møller Institute, The University of Southern Denmark, Odense 5230, Denmark, e-mail: (err, fh, wkj, lebo, norbert)@mmmi.sdu.dk.

P. Manoonpong is with the Embodied Artificial Intelligence and Neurorobotics Laboratory, SDU-Biorobotics section, The Mærsk Mc-Kinney Møller Institute, The University of Southern Denmark, Odense 5230, Denmark, and with the School of Information Science and Technology, Vidyasirimedhi Institute of Science and Technology, Rayong 21210, Thailand, e-mail: *poma@mmmi.sdu.dk, corresponding author.

Manuscript received XXX; revised XXX.

[1]SMOOTH: Seamless huMan-robot interactiOn fOr THe support of elderly people, http://smooth-robot.dk/

user adaptation to achieve smooth human-robot interaction and have various relevant applications outside elderly care facilities. For example, robots could serve drinks and snacks at social events as well as guide people to navigate around hospitals, airports, museums, conference venues, hotels, etc.

Robotic technology for healthcare has undergone considerable development in the last decades [1], [2], [3], but there are many limitations to the deployment of robotic solutions in this sector such as the high cost, safety, and, arguably the most important aspect, poor acceptance by the elder population. Some key elements to improve acceptance of healthcare robots are their functionality and real-time adaptability for individual users in human-robot interaction [4]. This paper focuses on the aspect of robot adaptability to individual users of social welfare robots when guiding people in an elderly care center or a nursing home. Guide robots are typically driven by traditional control strategies [5], [6], [7], [8], [9], [10] which are not well suited to environments consisting of people with highly diverse mobility capabilities since existing methods lack proactivity and continuous online robot (motion/speed) adaptation to individual users. They are typically pre-programmed with specific (navigation) behaviors. Consequently, they often fail to effectively adapt their behavior on the fly to handle the changing needs (walking at different speeds) of their users (see also the Related Work section).

This paper presents our advances on the development of a proactive control architecture to implement efficient guiding of people (i.e., our first use case, Fig. 1) by our SMOOTH robot (Fig. 2). The proactive control for this scenario with robot speed adaptation consists of three main modules: navigation control, visual human detection, and temporal error correlation-based neural learning. The robot predicts human speed based on visual information and uses this prediction to continuously and proactively adapt its speed to individual users on the fly. The robot can basically learn the speed control parameter (speed gain) online during the guiding process. Therefore, it can autonomously and smoothly guide[2] the user to a target location without prior knowledge of personality and preferences (i.e., walking speed in this study) and without preliminary (offline) training. This novel approach is different from others which typically require this kind of prior knowledge [11], [12] and/or a prior training/learning process with a number of trials[3] (e.g., reinforcement learning [13], [14]) (see the Related Work section). The main contributions of our study are threefold.

- Firstly, we propose a proactive robot control architecture, integrating three main modules for robot navigation control, visual human detection, and fast online robot learning.
- Secondly, for fast online robot learning, we propose temporal error correlation-based neural learning to smoothly guide with individual user speed adaptation in a continuous manner without prior knowledge of the environment and human models.
- Finally, we validate the performance of the proposed proactive robot control for a welfare robot guidance scenario in different real-world environments with different users, including a resident of an elderly care center in Køge, Denmark (i.e., our end user).

[2]The guiding smoothness is considered by the continuous motion of the robot with a speed matching that of human walking to keep an appropriate distance from its user.

[3]Such a process is typically performed in simulation first, due to the number of trials [13], depending on the learning algorithm and control complexity. In contrast, our method with fast online learning can directly apply to a real robot.

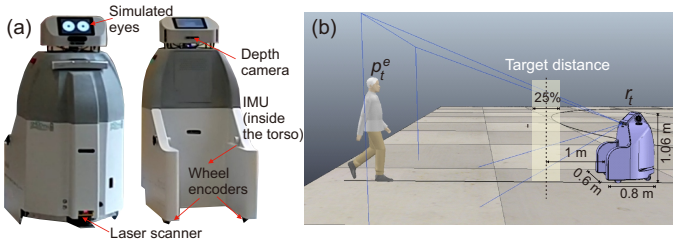

Fig. 2. SMOOTH robot and simulation environment. (a) Real SMOOTH robot with a multitude of sensory systems (described below). Here the four main sensors used in this study are depicted: Depth camera, laser scanner, wheel encoders, and inertial measurement unit. The camera is for human detection and used in temporal error correlation-based neural learning for robot speed adaptation. The other sensors are for navigation control. The update frequency of the robot, limited by the camera system, is approx. 10 fps (Hz) which is sufficient for our use case. This is due to the fact that the average target-human walking speed for robot guiding here is usually slow. It is between 0.2 m/s (elderly people) and 1.1 m/s (young people). (b) Simulation of the SMOOTH robot and a target distance with a 25% acceptable deviation range between the robot and the follower (i.e., 1 ± 0.25 m). The distance with a deviation range was also suggested by caregivers at an elderly care center as a safety factor for guiding elderly people to provide sufficient space when guiding an elderly person with a wheeled walker. It is also considered as "far phase" personal distance of the proxemics model [15]. p_t^e represents the Euclidean distance between the human and robot with respect to the robot position r_t.

Taken together, this study covers a wide range of research from robot control technology development to technological validity in a relevant environment (inside a building) and a system prototype demonstration in an operational environment (Danish elderly care center). The rest of the paper is structured as follows. Section II presents a review of related work in healthcare robot adaptation for individual users. Section III presents the SMOOTH robot system including its hardware, simulation, and proactive control for individual user adaptation towards smooth human-robot interaction. The SMOOTH robot hardware has been developed and used as an experimental platform for this SMOOTH project. The proactive control consists of three modules for 1) navigation control, 2) visual human detection, and 3) temporal error correlation-based neural learning. Section IV presents the results obtained from our experiments in simulation and the real world, together with a final test performed at a Danish elderly care center with an elderly resident. Finally, section V presents a discussion and conclusion on the main results of the paper together with the future scientific steps proposed for the project.

II. Related Work

Healthcare robotics is a general term which includes, among others, rehabilitation robotics, companion robots, and social robots with applications for elderly care [3], [16], [17]. Of these, social healthcare robots have the potential to deliver a higher impact on society since they can support an independent

life for the elder population as well as relieving pressure on caregivers [18]. To enhance user experience and acceptance, healthcare robots and, in general, socially assistive robots, are nowadays witnessing a shift toward including adaptation of their behavior to individual users through various approaches including user profiling in cognitive architectures [19], building relations with the user [10] or data-driven models [20], and adaptive reinforcement learning [13].

Many of the technological and methodological needs of service and healthcare robotics have already been addressed, yet some environments, like hospitals, require special techniques, such as for localization purposes [21], [22], given their typical physical structure with long corridors and few landmarks. Yet, the need to adapt the behaviour of healthcare robots became evident in one of the pioneering robots in the field, robot Pearl [23]. Pearl was developed as a mobile platform to support the elderly at home and in nursing homes. Its main purpose was to provide the elderly with reminders of their daily activities, successfully adapting the way of providing the reminders to avoid annoyance to the user. Another functionality of Pearl was to help the elderly navigate their environments, yet, in this case, there was no adaptation of the robot speed since it was pre-programmed with a constant speed, making it too fast or too slow depending on the user. Another significant work in assistive robots for the elderly is Care-O-bot [24], which can be used as a walking aid, and to execute fetch and carry tasks. The walking aid mode can be seen as a rollator, where the robot is physically controlled by the user, but it can also plan collision free paths which can be modified by the user through the application of pressure on the handles, solving the problem of changing the speed through a shared control mechanism. The work in [11] presents a guide robot which adheres to proxemics rules, keeping an appropriate distance from the users, and adapting its behavior according to whether or not the human is engaged in the guiding process. In this work, the robot adapts its speed using a proportionality mechanism with the predefined proxemics rules. It is triggered by the proximity to the human, which can be behind or on the side of the guiding robot. Adaptation to human body language has also been studied for assistive robots [25]. This work combines a quadrupole-based navigation planner with a slippage controller to develop a robot that can accurately perform navigation tasks commanded by the user through gestures.

Adaptation in healthcare and assistive robots has become an important research topic, and focuses on other aspects of interaction between robots and users, apart from guiding. However, these techniques typically require user profiling; gathering information about the personality and preferences of the user to inform and shape the robot behavior [12]. For instance, the work in [14] investigates the effect of matching the personality of a rehabilitation robot and the user. Furthermore, this work uses reinforcement learning to adapt certain parameters of robot behavior (movement, coaching messages, and proximity) to maximize the performance of the user in the rehabilitation task. A planning-based algorithm for user adaptation in the context of assistance for dressing is presented in [26]. Starting with some default settings, and assuming the robot is endowed with the relevant behaviors to execute shoe dressing actions, this algorithm can adapt the speed of such actions and the level of information provided to the user based on user feedback.

While user profiling and the personalization of robot behavior clearly has its merits, it is not suited to tasks where adaptation must be fast and the ability to deal with unknown individual users is required. On the other hand, user adaptation without profiling relies on fixed reactive control, modification of planners and shared control mechanisms which have limitations in terms of adaptability. Typically, reactive control with fixed/predefined control parameters [23], [27] can stably and smoothly adapt robot behavior (e.g., robot speed) to cope with a small range of human behavior variations (e.g., a small range of different walking speeds). Most works that rely on changes to planning mechanisms for guidance focus on social interaction aspects [28], [29], [30] and omit adaptation to the user speed. One notable exception is the work presented in [20] where the authors propose a modification of the cost of planning algorithms which allows a robot to guide a person with a closer average distance regardless of the person speed. Although their system adapts to several human speeds the adaptation term in the cost is data-driven, i.e., learnt from examples, and therefore requires trajectory examples which might not match the human speed. Alternatively, a standard stop-and-wait behavior strategy is employed [5], [31] while shared control [32], [33], [34] requires most user involvement in the robot movement (i.e., a tightly coupled human-robot system [35]). Thus, these approaches are not appropriate in our scenario here for the following reasons: 1) it has to deal with a wide range of walking speeds (e.g., very slow 0.2 m/s to fast 1.1 m/s), and 2) it requires less human involvement or less human intention (loosely coupled) for robot adaptation. This work presents a proactive control architecture that avoids profiling and data-driven adaptation (i.e., it adapts faster without user data), does not rely on predefined control parameters (i.e., parameters adapt to specific users), nor on tight human-robot coupling, all of which is achieved by integrating online learning for adapting quickly and flexibly to individual users with various walking speeds in healthcare applications.

III. The SMOOTH robot system

In this section, we describe the SMOOTH robot system. First, the robot hardware and its 3D physical simulation are provided, followed by the proactive robot control which is the main contribution of this study.

A. Robot Hardware and Simulation

1) SMOOTH Robot Hardware: We developed a robotic platform (called SMOOTH) with the ability to address different common use cases in elderly care centers (Fig. 2(a)). The design and development of the robot by the consortium of the SMOOTH project consists of a mobile base, torso, and head. The robot measures 0.8m (length) x 0.6m (width) x 1.06m (height) (Fig. 2(b)). The mobile base is a three-wheeled robot platform with two actuated wheels at the back and a caster wheel at the front. The base also contains a safety laser scanner (Hokuyo UAM-05LP-T301) covering 270° at the front, wheel

encoders, and an inertial measurement unit (IMU, MPU-9150 9-axis with integrated gyro, accelerometer, and compass sensors) for autonomous navigation purposes. The torso of the robot contains a mini PC (Intel®NUC, 2.4 GHz Intel Core i3-7100U Dual-Core), two depth cameras (Intel®RealSense D435, one each at the front and back), an array of microphones and speakers for speech synthesis and recognition. The head includes two touch screens for user interface and simulated eyes[4], and four depth cameras (Intel®RealSense D435, one each at the front, back, and on either side) for object/human recognition. In this study, only the back camera is used for human speed prediction and robot speed adaptation. The hardware system uses the Robot Operating System (ROS) as a bridge for communicating, operating, and synchronizing software packages between the different computing nodes of the system. The entire SMOOTH robot system including the mini PC for implementing our proactive robot control (Fig. 3) consumes approx. 120 watts, which is supplied by a 24V, 40Ah lithium iron phosphate battery (LiFePO4). The average run time on a fully charged battery is 8 hours. Further details of the SMOOTH robot can be found in [39].

2) SMOOTH Robot Simulation: We simulate the SMOOTH robot using the 3D physical simulation framework (called V-REP, currently integrated into the new robot simulator CoppeliaSim[5]) with the Bullet physics library. The simulation environment is used for developing our proactive control and preliminary test before transferring it to the real robot. The robot model (Fig. 2(b)) is qualitatively consistent with the real one (Fig. 2(a)) in the aspects of geometry, mass distribution, motor torque/speed, and sensors. The CAD model of the robot is imported into the simulation scene and used as the dynamic model for simulation experiments. The robot wheel motors are simulated by torque/force mode joints and the depth camera is simulated by a vision sensor with RGB and depth information. Here, we add Gaussian-distributed noise with a standard deviation of, e.g., 5% to sensor signals. The model of a walking person is provided by the simulator (i.e., Bill on path). The model aims to resemble natural human walking behavior with the potential to vary instantaneous walking speed. In our experiments (described below), both the robot and person are assigned to predefined paths.

B. Proactive Robot Control

To achieve individual user adaptation in a robot guidance scenario, we propose proactive robot control (Fig. 3).

It consists of three main modules: navigation control, visual human detection, and temporal error correlation-based neural learning. The navigation control module is for autonomously navigating and guiding the user to a given location. When navigating the environment, if the robot detects an obstacle in its path, it will consider obstacle avoidance as the highest priority. As such, the robot will automatically and gradually decrease its speed to avoid the obstacle during guiding. The visual human detection module is for detecting human movement, translating it into the distance between the human and robot, and thereby predicting human walking speed. The neural learning module is for online learning to adapt the robot speed to individual human walking speed to maintain the distance during guiding (i.e., 1 m with an acceptable deviation range of 25%). This online learning approach does not require human or environmental models or prior knowledge of human walking speed preference. Instead, it relies only on visual human detection to adapt the robot speed. Note that, among these main modules, the visual human detection is the most computationally expensive part (highest control effort) while the neural learning has the cheapest computational cost (lowest control effort). The details of each module are described below. In section IV, we experimentally show the stability and robustness of the closed-loop proactive control system under different conditions (including different light levels and dynamic environments (see also Supplementary Figures 1-3)), which relies on the robustness of the human detection module, the stability of the navigation control module, and the stability results of the neural learning mechanism [40] (see also Supplementary Figure 4).

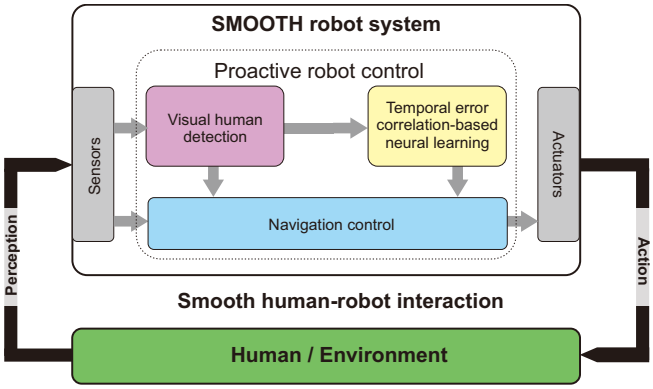

Fig. 3. Proactive control architecture for online individual user adaptation. The proactive control operates in a so-called embodied sensorimotor loop for smooth robot guiding behavior generation and smooth human-robot interaction. Note that we call our approach proactive control since its neural learning mechanism correlates two kinds of input signals (predictive and reflex) with different time steps (or scales), finally using the predictive signal to proactively control or modulate the robot speed.

1) Navigation Control: We developed navigation control to allow the SMOOTH robot to navigate in an indoor environment by moving to a given target location while avoiding obstacles in its path. It is based on a state-of-the-art mobile robot navigation system (i.e., the ROS navigation stack [41]) that basically transforms odometry and sensor information into safe velocity commands for a given robotic platform. For the purposes of this study, we have extended the navigation system using two main components: the Waypoint server to define a target in a practical way and the command adaptor for robot speed adaptation (described below). Figure 4 shows the architecture of our ROS-based navigation control.

The navigation control consists of two separate functionalities: self-localization and velocity control in the respec-

[4] The simulated eyes enable people to establish eye contact [36]. The design of the eyes in round shape follows human-robot interaction principles [37] aiming for acceptance and trust [38]. Although the eye contact has not been used during guiding in the study, we have recently explored the use of eye contact for trust, friendly human-robot interaction in other tasks, like serving drink.

[5] http://www.coppeliarobotics.com/

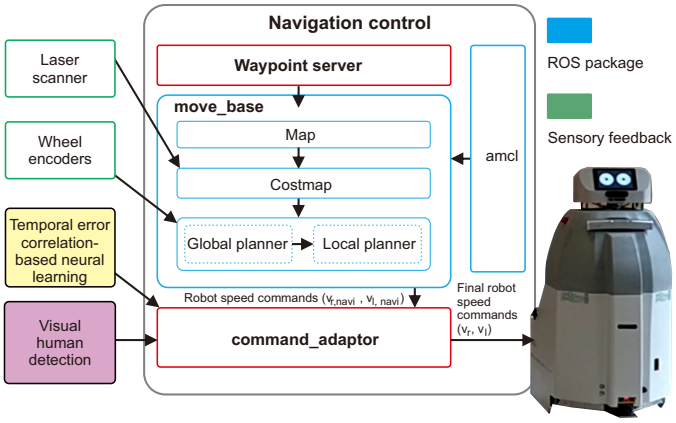

Fig. 4. Navigation control architecture for autonomous in-door robot navigation, obstacle avoidance, and human guidance with a human-centered adaptive strategy. Sensory feedback is shown by green squares, packages from ROS by blue squares, and additional components by red squares. The outputs (right $v_{r,navi}$ and left $v_{l,navi}$ motor speeds) from the navigation control for goal achievement are further modulated by the output of the neural learning through the command adaptor for robot speed adaptation with respect to human walking speed. Additionally, visual human detection will stop the robot motion (i.e., setting $v_{r,l,navi}$ to 0.0 through the command adaptor) if the human disappears during guiding. The final right v_r and left v_l motor speeds are sent to the robot.

tive *amcl* and *move_base* packages. These processes use the sensory data of the robot (laser scanner and wheel encoders (Fig. 2(a))) to encode the actual environmental information into a probabilistic pose, represented by an internal map. The self-localization, *amcl*, is based on the probabilistic Monte Carlo localization approach [42]. The velocity control, *move_base*, uses information from the environment with a previously created *Map* and sensory information from the laser scanner in the form of a *Costmap* to generate a series of velocity commands through the interaction between the global planner and local planner. The global planner uses the Dijkstra algorithm [43] to output the shortest route in the internal map given an initial position and a goal position. The local planner uses the Dynamic Window Approach (DWA) algorithm [44] to generate an optimal combination of feasible and safe velocity commands in the instantaneous position of the robot within constraints of the robot and environment. The laser scanner sensor receives proximity information to update obstacles in the environment into the *Costmap*, and the local planner then uses this updated layout to determine the trajectory of the robot. Finally, the local planner selects the optimal velocity commands of the right $v_{r,navi}$ and left $v_{l,navi}$ motor speeds to drive the robot from the current position to a position close to the global planner trajectory while avoiding obstacles in its environment (Fig. 5). In this study, the anticipation of an unexpected human motion in an obstacle avoidance situation is not integrated in the local planner. However, as a safety factor during the guiding task, we define the target distance between the human and robot to 1 ± 0.25 m, limit the robot maximum speed to a low value of 1.5 m/s, and configure the robot to only drive forward or stop (positive or zero speed command) where driving backward is allowed only in a certain condition with manual control. This minimal approach will allow the human to react (e.g., slow down walking speed or stop) in time during obstacle avoidance. While the current navigation control can allow the robot to avoid obstacles in both static environments (Fig. 5) and dynamic environments (Supplementary Figures 1-3), dealing with multiple dynamic obstacles will require more advanced motion planning [45], [46] and go beyond the scope of this study.

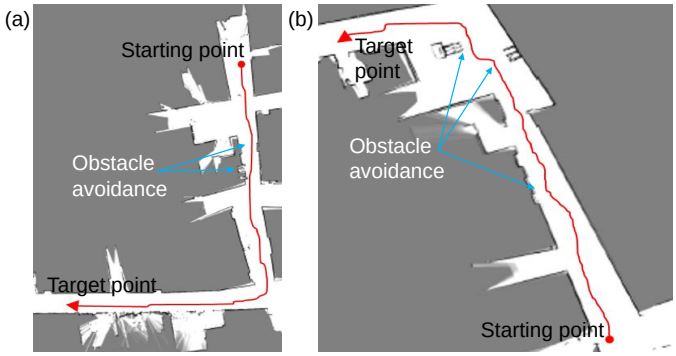

Fig. 5. Examples of autonomous navigation with obstacle avoidance. (a), (b) The robot was set to autonomously navigate from two different locations inside the SDU building. The distances traveled were approximately 30 and 60 meters, respectively. The robot successfully navigated 100% over five runs in each case.

For practicality, we developed and integrated the Waypoint server node (red box in Fig. 4) into the navigation stack. The user can store the pose of the robot in the created map with an ID name. Afterward, the user can select the different locations in the map defined by its ID (for instance, ID “dining room”, ID “living room”, or ID “laundry room”) as target locations. This utility allows the user to simply define a target location for the robot in an elderly care center, e.g., the dining room.

For online robot speed adaptation to match the walking speed of an individual user (including elderly subjects) during autonomous navigation and guidance, we developed the command adaptor (red box in Fig. 4). This piece of software uses the output of the neural learning (described below) to modulate the motor speeds $v_{r,l,navi}$ generated by the navigation control. As a result, the robot autonomously navigates and adapts to the pace of the user, avoiding obstacles as predicted. The system also considers human detection as a priority task. If the user stops and its position is outside a certain range, the robot starts to call the user to encourage him/her to continue walking toward the goal (not investigated here).

2) Visual Human Detection: The human detection system is tasked with to estimating the 3D position p_t of each human in the field of the camera’s view. This is done by first detecting the 2D pose of each human in the RGB image using CenterNet [47] in the multi-pose configuration. CenterNet is used here since it is a state-of-the-art method for real-time object detection. Such a detected pose can be seen in Fig. 6. The next step is to use the available depth information to project the detected joint locations in 3D, resulting in a 3D skeletal representation for each detected person. From this 3D representation, p_t and other information such as torso direction can be extracted. One way to estimate p_t would be to find the average or median joint position in the skeleton. However,

such an approach might result in instability since joints along extremities are not always found by CenterNet, leading to large jumps in the average measurements from frame to frame. To ensure robustness, only the shoulder joints are used. A torso point is sampled halfway between the image coordinates of the two shoulder joints, and projected to 3D. This 3D torso center is then set as p_t. The torso direction is also extracted by finding the vector orthogonal to the vector between two shoulder joints, which is also parallel to the ground plane.

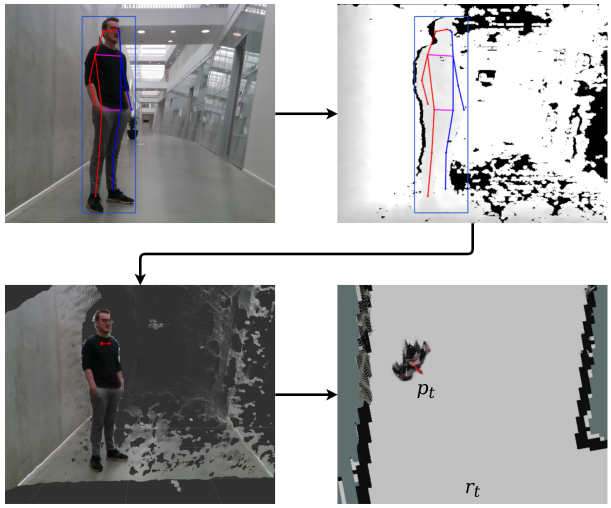

Fig. 6. Visual human detection using human pose estimation CNN. First the pose of each person in the frame is found using the CNN. The detected shoulder joints are then projected to 3D using the available depth information. These 3D locations are then used to find the center torso position and orientation, by finding the vector orthogonal to the vector between the shoulder joints, parallel to the ground. The detected 3D human position p_t is shown on the map, relative to the robot position r_t. After obtaining p_t, it is transmitted to the temporal error correlation-based neural learning circuit described in the following section.

We validated the robustness of the human detection system by testing it in three different light conditions: bright ($\approx$ 315 lux), medium ($\approx$ 185 lux), and dark ($\approx$ 15 lux). The experiment was conducted in a room with ceiling lights and big windows at midday. For the bright condition, the ceiling lights were on and the curtains were up. For the medium condition, the curtains were down but the ceiling light was on. For the dark condition, the curtains were down and the ceiling light turned off. The result shows that the detection rate of the human detection system is 100% in the three different light conditions. The detection rate is defined as the percentage of the sample size (here, 190) where the detector outputs a correct bounding box around the person and no other bounding box.

While the human detection system can detect each person in a frame, it does not recognize which detection correlates to the person being guided. To deal with this issue, we apply the face recognition model FaceNet [48]. FaceNet is a CNN, trained to project cropped face images into a 128-dimensional vector space encoding. In this space, face encodings of the same person are clustered together, while the encodings from different people are spaced out. A person can thereby be recognized by comparing the encoding to clusters of encodings from known people. At the start of the guiding process, face images of the person being guided are encoded, by cropping them using the detected facial keypoints from CenterNet. Hereafter, the face of each detected person is encoded and compared to the encodings of the guided person using a threshold of the L2-norm. Examples of human face recognition can be seen at Supplementary Figure 5. Note that since the visual human detection used is based on the standard CenterNet and FaceNet, it only supports proactive control and is not a key contribution to this study. We refer to [47], [48] for further evaluation. Although the described vision system can provide several features in this case (human detection, human-robot distance estimation, and human face recognition), it is still unable to identify human beings. To accomplish this, we can enhance our robot sensing system with additional sensors such as a thermal camera for sensing human body temperature [49], [50] and an ultra-wideband (UWB) radar for sensing human vital sign signals (e.g., respiration and heartbeat) [51], [52].

3) Temporal Error Correlation-based Neural Learning: The processed visual information described in the previous section is fed into the temporal error correlation-based neural learning circuit (Fig. 7) to modify a plastic synapse (comparable to speed gain control) during learning. The learning goal in this study is to enable the robot to quickly learn to adapt its moving speed to match human walking speed in an online manner. In this way, the robot can perform simplified smooth human-robot interaction in the guidance scenario. To achieve this, we propose here for the first time, a temporal error correlation-based neural (TEC) learning rule, derived from a combination of input correlation (ICO) learning [40] and error-based (Widrow-Hoff) learning [53]. It basically correlates two temporal input signals at different time steps (Fig. 7). Inspired by biological motor learning [54], [55], [56], [57], in this study we use temporal prediction errors (e_t, e_{t-1}) as our two-time step input signals. The first time-step input signal is the current prediction error e_t. It is defined as $e_t = p_t^e - p_i$, where p_t^e is the Euclidean distance between the human and robot (calculated from the 3D human position p_t, described above), with p_i being the ideal target distance (e.g., 1.0 m, Fig. 2(b)). The second time-step input signal is the previous prediction error e_{t-1}. The learning circuit uses the two input information to predict human walking speed and generates a proper output F to modulate robot speed commands, originally generated by the navigation control (Fig. 4).

According to the ICO learning, the connection w_t of a predictive signal (i.e., here the current prediction error, e_t) is initially given with zero strength. In this situation, the robot moving speed will be modulated only by a constant reflex signal (i.e., here the previous prediction error signal, e_{t-1}). Over time, the correlation between the predictive and reflex signals will adapt the synapse w_t, connecting the predictive signal with the learner neuron. Consequently, after a few trials (depending on signal correlation) during the learning phase, the robot speed will finally be driven by the predictive signal instead. The learning algorithm applied has the property that learning will stop when the change in the reflex signal is zero [40]; i.e., when the moving speeds of the robot and the human match. Since the learned weight is stored, the next time the robot detects the same person using the visual face recognition method (described above, Supplementary Figure 5), it will

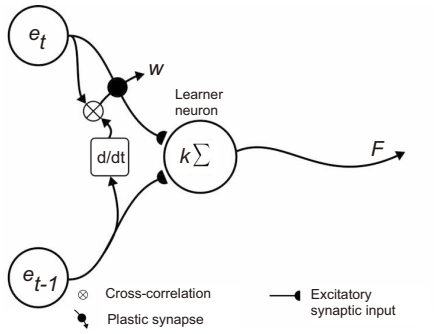

Fig. 7. Temporal error correlation-based neural learning circuit. The temporal errors, calculated from the prediction error of the human position and the target position and the previous prediction error, are fed into the circuit to calculate a proper speed modulation factor F_t for adapting the robot speed to match human walking speed. The weight (or adaptive speed gain) of the predictive signal (error prediction, e_t) is adjusted according to the learning rule (Eq. 1) to obtain F_t for robot speed adaptation. Using the predictive signal allows the robot to adapt its speed in a stable and proactive way [58], [59].

retrieve the learned weight as an initial speed gain value which can be continuously and quickly adapted on the fly during guiding when the person changes speed. The TEC learning rule for the weight change is given by:

$$\Delta w_t = \mu e_t \frac{\Delta e_{t-1}}{\Delta t}, \tag{1}$$

where μ is a learning rate which defines how fast a system can learn. One could consider μ as the susceptibility for a synaptic change, which in a biological agent would be defined by its evolutionary development, which determines the agent's ability to learn a certain task. In this learning rule, only the plastic synapse w_t is permitted to change while the synapse of the reflex input is set to a positive value, e.g., 1.0. Note that w_t can be considered as an adaptive speed gain in robot speed adaptation. Formally the learning circuit produces its output F_t driven by:

$$F_t = k(e_t w_t + e_{t-1} 1.0), \tag{2}$$

where k is an amplifier factor (e.g., 2.0). The neural learner output F_t acts as a speed modulation factor which modulates robot speed commands as:

$$v_r = v_{r,navi} - F_t, v_l = v_{l,navi} - F_t, \tag{3}$$

where $v_{r,l}$ are the final speed commands to the right and left robot motors. $v_{r,l,navi}$ are the original speed commands to the right and left robot motors generated by the navigation control (Fig. 4).

As previously mentioned, the changing weight w_t only stabilizes when a zero change occurs in the tracking error, corresponding to the zero difference between the human position and target position. This also implies that the relative speed between the robot and human is zero, meaning the speed of the learning system has been matched with the speed of human tracking (Eq. 1). Figure 8 illustrates this effect. It shows the numerical simulation results of the learning system at different target (human walking) speeds (e.g., 1.0 m/s and 5 m/s). The system was initialized with its weight, speed, and prediction error at zero. When the speeds of the system and the target are different, the derivative of the reflex signal $\frac{\Delta e_{t-1}}{\Delta t}$ becomes a non-zero value. Therefore, the system starts to update its weight according to the TEC learning rule. The system is stable when the derivative is zero, meaning that the system speed matches the target speed or the speed of the tracking process.

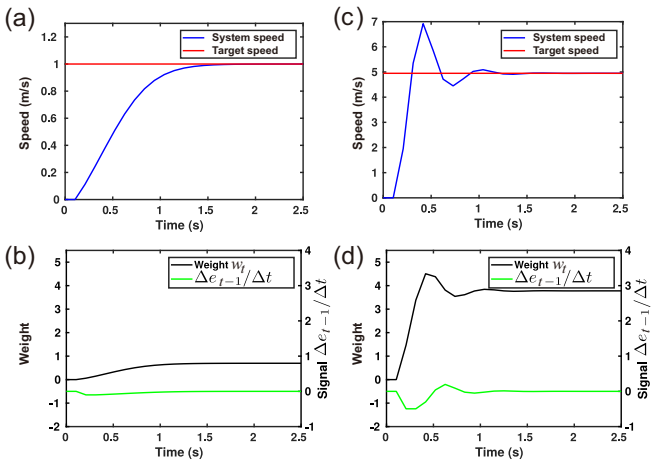

Fig. 8. Examples of the neural learning process. (a), (b) Numerical results of the process (Eq. 1) at a target speed of 1.0 m/s. (c), (d) Results of the process at a target speed of 5.0 m/s. The update frequency of the simulation was set to 10 Hz. Note that the system speed has no overshoot in case of a low target speed of 1.0 m/s because the control parameter (i.e., update frequency $(1/\Delta t)$ see Eq. 1) was properly adjusted. However, this frequency setup was a bit low for a high target speed (e.g., 5.0 m/s) causing an overshoot in weight and speed changes. However, after the overshoot, the system can converge to a certain weight and reach the target speed. This shows that the stability of the learning process.

IV. Experiments and Results

In this section, we analyze and evaluate the performance of the proactive robot control (an integration of the aforementioned modules (navigation control, visual human detection, and neural learning), Fig. 3) for a proactive guidance strategy. The strategy will allow the robot to autonomously navigate in different environments while at the same time quickly adapting its speed to that of the human target for smooth guidance. Four main experiments were carried out. The first and second experiments were performed in a 3D simulation environment to analyze the performance of the proactive control using different control parameters (i.e., adaptive versus fixed speed gains) and different guidance scenarios (i.e., guiding along a circular path, guiding with multiple turnings, guiding with curve turning), respectively. The third experiments were conducted to test the control of the SMOOTH robot (Fig. 2(a)) in a relevant real-world environment with two different subjects and paths. The final experiment demonstrated the functionality of our control system in an operational real-world environment (i.e., an elderly care center) with a real use case of guiding an elderly resident. It is important to note that for safety in all real

robot experiments[6], the SMOOTH robot was operated under several safety mechanisms. For example, the safety approved laser scanner sensor we used for navigation control counts with safety marking for collision detection. In case of emergency or critical failure, the robot will be immediately stopped or switched off by an emergency-stop-push button located at the robot torso. The robot maximum speed was limited to 1.5 m/s. Additionally, the robot will be in a standby mode in case of interruption or no change of the visual detection system. Note that, the control system will be unable to update the robot's speed as fast as the target (human) moves during the emergency or standby period. As a result, when the robot is allowed to move again, there could be an overshoot at the beginning (like the case shown in Fig. 8(c)). The overshoot can be avoided by introducing time-based decay in Eq. 1 to gradually reduce the adaptive gain over time.

A. Simulated Robot Experiments

In experiments I and II, the 3D simulation environment was setup as follows. A human model was initially placed 3.5 m behind the robot (Fig. 2(b)). The robot and human models were assigned to follow certain paths. The human walked with an average walking speed of 1.1 m/s. For our robot guidance here, we let the human follow the robot from behind since in our real use case at an elderly care center the walking path there is narrow and caregivers suggested the leading-following guiding strategy for safety instead of walking side by side.

1) Experiment I (adaptive vs fixed speed gains): Here, we used a straight path to compare the performance of the proactive control with an adaptive gain w_t versus fixed gains[7] w_{const}. The performance was evaluated in terms of the different distances between the robot and follower/human (i.e., robot-human distance). The adaptive gain was adjusted online through the TEC learning rule (Eq. 1) while the two fixed gains were predefined. They were set by scaling an optimal gain value up and down (i.e., convergent adaptive gain) with a certain factor (e.g., 3.0), as high $w_{const,h}$ and low $w_{const,l}$ fixed gains, respectively.

Figure 9 shows the experimental results with a comparison of an adaptive gain w_t, a high gain of 6.0 $w_{const,h}$, and a low gain of 0.67 $w_{const,l}$. Each case was repeated ten times and the average and standard error values of the robot-human distance are shown.

It can be observed that the adaptive gain with an initial value of zero quickly converged to an optimal value of 2.0 within 20 seconds (Fig. 9(a)). After convergence, the robot-human distance was also stably maintained at a target value of 1 m

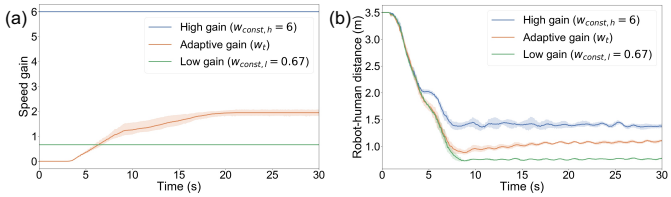

Fig. 9. Results of simulation experiments with adaptive and fixed gains. (a) Different control parameters (adaptive speed gain, fixed high speed gain, and fixed low speed gain). The adaptive gain was automatically adjusted to adapt the robot speed online during guiding such that the robot-human distance was maintained at around 1 m. (b) The robot-human distances of all the three parameter setups.

(Fig. 9(b)). As previously mentioned, the target value with a 25% acceptable deviation range was considered by caregivers at an elderly care center as a safety factor for guiding elderly people as well as providing proper clearance when guiding an elderly person with a wheeled walker. In contrast, use of the low fixed gain results in a short robot-human distance of around 0.5 m. This is too close and outside the safety range for guiding. Use of the high fixed gain results in a large robot-human distance of around 1.5 m. This is a bit too far and inconvenient if human-robot conversation is employed [64].

The resulting too-close and too-far robot-human distances when using fixed lower and higher speed gains are due to the following reasons. A fixed high speed gain causes an abrupt change in the robot speed abruptly (i.e., fast acceleration and deceleration). Thus, the robot will perform a stop-and-go motion pattern which can be observed by high ripples of the robot-human distance value (blue line in Fig. 9(b)). Consequently, the robot will maintain a far robot-human distance. On the other hand, a fixed low speed gain causes the robot to gently change speed. This makes the robot slower to react to the human when approaching. This will lead to a smoother guiding motion (low ripples in the robot-human distance value, green line in Fig. 9(b)) and finally converge to a close robot-human distance. Our online adaptation balances this by automatically finding an optimal speed gain (orange line in Fig. 9a) without knowing the human walking speed. It predicts human walking speed based on the robot-human distance over time and adapts its speed to achieve the best distance accuracy (orange line in Fig. 9(b)) compared to the fixed gains (i.e., conventional reactive robot control [60], [61]).

2) Experiment II (different guidance scenarios): Here, we investigated the robot online speed adaptation under different guidance scenarios, including guiding along a circular path, guiding with multiple turnings, and guiding with curve turning. Figure 10 shows the experimental results of the human and robot speeds as well as robot-human distance during guiding in each scenario. Each scenario was repeated ten times and the average and standard error values of the robot speed and the robot-human distance are shown.

For the circular path (Fig. 10(a)), we show the speed and robot-human distance profiles from the beginning where the robot speed was initially zero and the robot-human distance was 3.5 m. The robot adapted its speed to the human walking speed within 15 s. During that period, the robot-human

[6]In all experiments with humans, a written informed consent form was obtained from all participants. The consent form was adjusted continuously during the project according to the results of robot technology development. The experiments were performed in accordance with the ethical standards laid down by the 1964 Declaration of Helsinki and we followed the relevant basic principles of this declaration. Given the conditions explained above, the experiments do not need explicit approval by the Danish Research Ethics Committee, but the project was initially presented and discussed with the Committee.

[7]It is important to note that the fixed gain control is in principle a conventional robot reactive control method [60], [61], widely used in various robot behavioral adaptation tasks [62], [63]. Thus we basically compare our adaptive method with the conventional one.

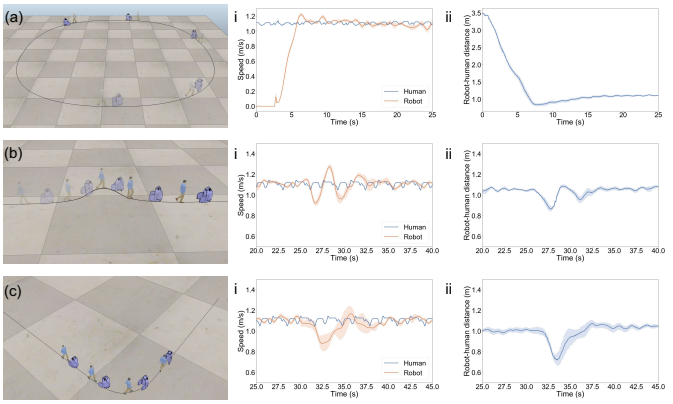

Fig. 10. Results of simulation experiments with different guidance scenarios. (a) Guiding along a circular path. (b) Guiding with multiple turning. (c) Guiding with curve turning. The robot and human speeds (i), as well as the robot-human distance (ii) of each scenario, are shown. In case of multiple turning and curve turning, the robot first decreases its speed when approaching the curve while the human still walks at a normal speed. Therefore, the relative speed decreases (robot speed - human speed), resulting in a decrease of robot-human distance (i.e., the Euclidean distance with respect to r_t, see Fig. 2). Note that all these scenarios were simulated using common situations which are likely to occur when implementing the robotic solution in the Ølby elderly center in Køge, Denmark (our end user). For example, the guidance scenario along a circular path is comparable to guiding an elderly resident to walk (cardio exercise) inside the center. Guiding with multiple turning can be considered as avoiding an obstacle on the path. Guiding with curve turning is a typical situation for guiding an elderly resident from the living room to the dining room (see our experiment IV).

distance profile also decreased. Afterward, it converged to the target distance of 1.0 m and maintained that distance over time. For guidance with multiple turning and curve turning (Figs. 10(b) and (c)), we only show the snapshots of the speed and robot-human distance profiles around the turning periods. At turning points, the robot speed decreased and then quickly increased to match the human walking speed. At sharp turning, e.g., around 27 s as shown in Fig. 10(b), the robot speed had an overshoot before returning to match the human walking speed. The robot-human distance profile also shows a similar pattern. The overshooting effect is because, in the simulation, the human walked with a constant speed while the robot decreased its speed during turning. Thus, the robot-human distance quickly decreased (i.e., large error). Consequently, the learning mechanism quickly sped the robot through the adaptive speed gain to maintain the target robot-human distance.

In all scenarios, the proactive control manages to adapt the robot speed to match the human walking speed (i.e., 1.1 m/s) and maintain the robot-human distance at around 1 m constantly, except for the second and third scenarios where the distance slightly decreased and increased due to the turning effect described above. However, it is still in an acceptable deviation range (i.e., 1 ± 0.25 m).

B. Real Robot Experiments

1) Experiment III (relevant real-world environment): We performed two different guiding tests in the corridors inside a building with two different trajectories and two human subjects (subject 1 and subject 2). Each test was repeated three times to explore the stability and adaptability of our proactive control system in the real world. The first trajectory for subject 1 has 60 m length with narrow corridors and a 90-degrees sharp curve (see Figs. 11(a) and (d)). The second trajectory for subject 2 is 30 m in length with a 90-degrees wide curve (see Supplementary Figure 6). The experimental result of the first trajectory is shown in Figs. 11(a), (b), (c), and (d) which present snapshots of robot guidance in the real-world environment, change in an adaptive gain, change in robot-human distance, and a map of the facility used for navigation along with the robot position during the guidance experiment, respectively. For the result of the second trajectory, we encourage readers to see Supplementary Figure 6.

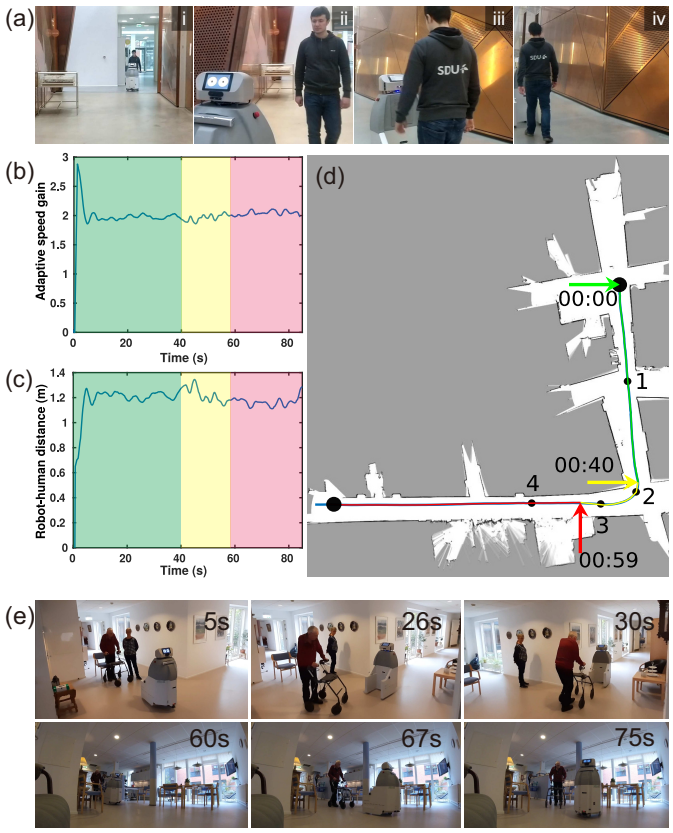

Fig. 11. SMOOTH robot guiding a subject over a distance of 60 m. (a) Snapshots of the robot guidance experiment (from left (i) to right (iv)). (b) Adaptive gain, adapted according to the TEC learning rule. (c) Robot-human distance. (d) Navigation map and robot trajectory. Note that real experimental artifacts are considered as variability in human walking and path planning for robot navigation. The green, yellow, and red colours in (b), (c), and (d) describe the different regions in the guidance map. The numbers depicted in (a) and (d) refer to the robot position during guiding. In this experiment, the adaptive gain was adapted online to adjust the robot speed to match the human walking speed of approximately 0.7 m/s. In the experiment, the robot experienced different light levels in a range of approx. 50-850 lux. We encourage readers to view a video of the experiment at www.manoonpong.com/ProactiveControl/video1.mp4. (e) SMOOTH robot successfully guiding an elderly resident at the Ølby elderly care center in Køge, Denmark. It smoothly guided him without a stop-and-go pattern from the living room to the dining room over a distance of 25 m. With SMOOTH proactive guiding, the robot adapted its speed to the human target (approximately 0.2 m/s) successfully establishing smooth human-robot interaction in a real case scenario. During the guiding task, the robot experienced different light conditions in a range of approx. 30 - 600 lux. We encourage readers to view the videos of this test at www.manoonpong.com/ProactiveControl/video2.mp4 and another test at www.manoonpong.com/ProactiveControl/video3.mp4.

In both tests (as shown in Fig. 11(a) and Supplementary Figure 6(a)), acceptable deviations occur from the target robot-human distance. For guiding subject 1, the robot-human distance was around 1.15-1.25 m (Fig. 11(c)), while for subject 2, the distance was around 0.8-1 m (Supplementary Figure 6(c)). The deviations are basically due to several unknown factors, including 1) complex interaction between different modules (navigation control, visual human detection, and neural learning) at different update frequencies, 2) environmental friction which was not included in the learning mechanism and the navigation control, and 3) a human walking pattern consisting of swing and stance phases. In the swing phase the human speed decreases, causing an increase in the robot-human distance while the opposite effect appears in the stance phase. This can be improved by considering human and environmental models. However, while not considering all unknown factors, the robot successfully achieved 100% guidance from the starting location to the end location over three runs for each test. Furthermore, it managed to online adapt its speed to match each human walking speed for smooth guidance without a stop-and-go motion, and maintain its distance to each subject within an acceptable range (i.e., 1 ± 0.25 m).

2) Experiment IV (operational real-world environment): Here, we finally demonstrate the functionality of the proposed proactive control system with a real end user at an elderly care center in Køge, Denmark. The task represented in Fig. 11(e) involves the guidance of an elderly resident with a trajectory of 25 m in length from the living room where the resident usually rests, toward the dining room. The robot successfully achieved the complex task (100% over three runs). In this task, it performed multiple functions including autonomous navigation through a real environment, obstacle avoidance, guidance, and online speed adaptation to match the resident's walking speed of approximately 0.2 m/s. For a comparison of the robot speed adaptation to individual users with different walking speeds, we refer to www.manoonpong.com/ProactiveControl/video4.mp4. This guiding use case has proven itself to be valuable for elderly and welfare environments as discussed in [39].

V. Discussion and Conclusion

In this paper, we present a novel proactive control approach for online individual user adaptation in a welfare robot guidance scenario. The approach combines three main modules for autonomous robot navigation, visual human detection, and online robot speed adaptation. The results show that the robot can navigate in different real-world environments and learn to predict human walking speed based on a distance function, such that it can autonomously adapt its speed to the user. Consequently, it can smoothly guide the user without a stop-and-go motion to the desired location while keeping its distance from the user at the target safety level (1 ± 0.25 m). Guiding without a stop-and-go motion (or without disturbing/interrupting human motion while following the robot) can lead to a higher degree of comfort[8].

[8]For service robots, comfort is considered as the ability of the robot to i) avoid disturbing the human with whom it shares the environment and ii) create trust on the user [38], [65], [66], [67].

Our approach was also successfully tested in an elderly facility where the robot smoothly interacted with an elderly resident (i.e., adapting its speed) and guided him from the living room to dining room over a distance of 25 m. If it encounters an obstacle on its way, the robot considers obstacle avoidance as the highest priority, automatically and gradually decreasing its speed to avoid the obstacle during guiding. Since the robot-human distance has been maintained at the target distance, the user can adapt his walking speed to the decreased robot speed accordingly. Once the obstacle has been avoided, the robot can smoothly return to guide the user at a normal speed (such a situation can be seen at www.manoonpong.com/ProactiveControl/video3.mp4).

In particular, with the control approach, the proposed temporal error correlation-based neural learning does not require the robot kinematic or environmental model for speed adaptation; it is generic and can be applied to other robot guiding systems [6], [7], [8], [9], [10] to achieve the same advanced feature. The approach does not need multiple learning trials for predicting human walking speed and adapting the robot speed. It can be implemented directly on a real robot for continuous online learning. This is different from conventional machine learning or data-driven approaches which usually require experimental data for training in simulation first before transferring the trained model into a real robot [13], [20]. Since our neural learning approach proactively adapts the robot speed to keep an appropriate distance from its user, the approach can be also applied in a reverse way to achieve smooth human following of a mobile robot. Typical existing human following methods relies on vision-based human tracking [68], [69], [70], [71] with conventional robot control (like, closed-loop PID control [71]). Thus, our method can enhance the human following methods by using the visual information to predict human position and online adapt a corresponding control gain as shown here.

The proposed individual user adaptability provides service robots with user-friendly, human-centered technology. The integration of this approach into our robotic platform SMOOTH increases the potential for exploring more complex human-robot interactions with multiple adaptive functions [5]. While the proposed approach is shown to be effective for individual user speed adaptation in a guidance scenario, several adaptive functions still need to be implemented to complete the guiding task to fully support elderly people. These adaptive functions include 1) adaptive speech recognition [72] allowing the robot to learn to recognize the speech of different users and turn toward the user upon request (i.e., asking the robot to guide), 2) adaptive smooth turning [73] and approaching [74], [75] the user to begin guiding, and 3) adaptive human-robot dialog [10], [76], [77] to keep motivating or encouraging the user (elderly person) during guiding to walk to a target location as well as to tell or warn the user to be aware of an obstacle on their way. These additional functions and the proposed guiding function in this study can be considered as robot primitives. They can be adaptively combined through action sequence learning methods [78], [79], [80] to obtain a complete effective solution for elderly people in a welfare robot guidance scenario.

As the control approach is a modular-based design, it is flexible and offers the future possibility of integrating more modules to implement adaptive speech recognition, smooth turning and approaching, and human-robot dialog functions. Thus, in future work, we will extend our control approach according to the aforementioned adaptive modules and test the robot extensively in facilities with multiple elderly residents and more complex interactions.

ACKNOWLEDGMENTS

The authors would like to thank the staff and residents at the Ølby elderly care center in Køge, Denmark for providing fruitful discussions, valuable insights, and robot tests. We would also like to thank Conny Heidtmann from MMMI/SDU for organizing and helping with the tests at the care center, as well as Christian Hauch and his team at Robotize Aps for technical support and robot development. We thank the SMOOTH project's partners for the overall project concept development and general technical discussion. This research was part of the SMOOTH project (project number 6158-00009B) by the Innovation Fund Denmark.

REFERENCES

[1] L. Bodenhagen, S.-D. Suvei, W. K. Juel, E. Brander, and N. Krüger, "Robot technology for future welfare: meeting upcoming societal challenges–an outlook with offset in the development in scandinavia," *Health and Technology*, vol. 9, no. 3, pp. 197–218, 2019.

[2] A. O. Andrade, A. A. Pereira, S. Walter, R. Almeida, R. Loureiro, D. Compagna, and P. J. Kyberd, "Bridging the gap between robotic technology and health care," *Biomedical Signal Processing and Control*, vol. 10, pp. 65–78, 2014.

[3] D. Portugal, P. Alvito, E. Christodoulou, G. Samaras, and J. Dias, "A study on the deployment of a service robot in an elderly care center," *International Journal of Social Robotics*, vol. 11, no. 2, pp. 317–341, 2019.

[4] L. D. Riek, "Healthcare robotics," *Communications of the ACM*, vol. 60, no. 11, pp. 68–78, 2017.

[5] T. Kruse, A. K. Pandey, R. Alami, and A. Kirsch, "Human-aware robot navigation: A survey," *Robotics and Autonomous Systems*, vol. 61, no. 12, pp. 1726–1743, 2013.

[6] P. Leica, J. M. Toibero, F. Roberti, and R. Carelli, "Switched control to robot-human bilateral interaction for guiding people," *Journal of Intelligent & Robotic Systems*, vol. 77, no. 1, pp. 73–93, 2015.

[7] H. Ishiguro, T. Ono, M. Imai, and T. Kanda, "Development of an interactive humanoid robot "Robovie"," in *IEEE Int. Conf. on Robotics and Automation*, 2003, pp. 1848–1855.

[8] J. Pineau, M. Montemerlo, M. Pollack, N. Roy, and S. Thrun, "Towards robotic assistants in nursing homes: Challenges and results," *Robotics and Autonomous Systems*, vol. 42, no. 3-4, pp. 271–281, 2003.

[9] H.-M. Gross, H.-J. Boehme, C. Schröter, S. Müller, A. König, C. Martin, M. Merten, and A. Bley, "Shopbot: Progress in developing an interactive mobile shopping assistant for everyday use," in *2008 IEEE International Conference on Systems, Man and Cybernetics*. IEEE, 2008, pp. 3471–3478.

[10] T. Iio, S. Satake, T. Kanda, K. Hayashi, F. Ferreri, and N. Hagita, "Human-like guide robot that proactively explains exhibits," *International Journal of Social Robotics*, pp. 1–18, 2019.

[11] A. K. Pandey and R. Alami, "A step towards a sociable robot guide which monitors and adapts to the person's activities," in *International Conference on Advanced Robotics*. IEEE, 2009.

[12] S. Rossi, F. Ferland, and A. Tapus, "User profiling and behavioral adaptation for HRI: A survey," *Pattern Recognition Letters*, vol. 99, pp. 3–12, 2017.

[13] G. Velentzas, T. Tsitsimis, I. Rañó, C. Tzafestas, and M. Khamassi, "Adaptive reinforcement learning with active state-specific exploration for engagement maximization during simulated child-robot interaction," *Paladyn, Journal of Behavioral Robotics*, vol. 9, no. 1, pp. 235–253, 2018.

[14] A. Tapus, C. Ţăpuş, and M. J. Matarić, "User—robot personality matching and assistive robot behavior adaptation for post-stroke rehabilitation therapy," *Intelligent Service Robotics*, vol. 1, no. 2, p. 169, 2008.

[15] E. T. Hall, "The hidden dimension," 1966.

[16] R. Bogue, "Europe leads the way in assistive robots for the elderly," *Industrial Robot: An International Journal*, 2017.

[17] H. Robinson, B. MacDonald, and E. Broadbent, "The role of healthcare robots for older people at home: A review," *International Journal of Social Robotics*, vol. 4, no. 6, pp. 575–591, 2014.

[18] S. Baumgarten, T. Jacobs, and B. Graf, "The robotic service assistant-relieving the nursing staff of workload," in *ISR 2018; 50th International Symposium on Robotics*. VDE, 2018, pp. 1–4.

[19] A. Umbrico, A. Cesta, G. Cortellessa, and A. Orlandini, "A holistic approach to behavior adaptation for socially assistive robots," *International Journal of Social Robotics*, pp. 1–21, 2020.

[20] D. Feil-Seifer and M. Matarić, "People-aware navigation for goal-oriented behavior involving a human partner," in *2011 IEEE International Conference on Development and Learning (ICDL)*, vol. 2. IEEE, 2011, pp. 1–6.

[21] X. Bai, Z. Zhang, L. Liu, X. Zhai, J. Panneerselvam, and L. Ge, "Enhancing localization of mobile robots in distributed sensor environments for reliable proximity service applications," *IEEE Access*, no. 7, 2019.

[22] Y. Dobrev, P. Gulden, and M. Vossiek, "An indoor positioning system based on wireless range and angle measurements assisted by multi-modal sensor fusion for service robot applications," *IEEE Access*, vol. 6, 2018.

[23] M. Montemerlo, J. Pineau, N. Roy, S. Thrun, and V. Verma, "Experiences with a mobile robotic guide for the elderly," in *AAAI/IAAI*, 2002, pp. 587–592.

[24] B. Graf, M. Hans, and R. D. Schraft, "Care-O-bot II—development of a next generation robotic home assistant," *Autonomous Robots*, vol. 16, no. 2, pp. 193–205, 2004.

[25] W. Yuan, Z. Li, and C. Su, "Multisensor-based navigation and control of a mobile service robot," *IEEE Transactions on Systems, Man, and Cybernetics: Systems*, pp. 1–11, 2019.

[26] G. Gerard Canal, G. Alenyà, and C. Torras, "Adapting robot task planning to user preferences: an assistive shoe dressing example," *Autonomous Robots*, vol. 43, no. 6, pp. 1343–1356, 2019.

[27] H. Gross, H. Boehme, C. Schroeter, S. Mueller, A. Koenig, E. Einhorn, C. Martin, M. Merten, and A. Bley, "TOOMAS: Interactive shopping guide robots in everyday use - final implementation and experiences from long-term field trials," in *2009 IEEE/RSJ International Conference on Intelligent Robots and Systems*, 2009, pp. 2005–2012.

[28] G. Bardaro, A. Antonini, and E. Motta, "Robots for elderly care in the home: A landscape analysis and co-design toolkit," *International Journal of Social Robotics*, pp. 1–25, 2021.

[29] R. Triebel, K. Arras, R. Alami, L. Beyer, S. Breuers, R. Chatila, M. Chetouani, D. Cremers, V. Evers, M. Fiore *et al.*, "Spencer: A socially aware service robot for passenger guidance and help in busy airports," in *Field and service robotics*. Springer, 2016, pp. 607–622.

[30] F. Del Duchetto, P. Baxter, and M. Hanheide, "Lindsey the tour guide robot-usage patterns in a museum long-term deployment," in *2019 28th IEEE International Conference on Robot and Human Interactive Communication (RO-MAN)*. IEEE, 2019, pp. 1–8.

[31] R. Kittmann, T. Fröhlich, J. Schäfer, U. Reiser, F. Weißhardt, and A. Haug, "Let me introduce myself: I am Care-O-bot 4, a gentleman robot," *Mensch und Computer 2015–proceedings*, 2015.

[32] S.-Y. Jiang, C.-Y. Lin, K.-T. Huang, and K.-T. Song, "Shared control design of a walking-assistant robot," *IEEE Transactions on Control Systems Technology*, vol. 25, no. 6, pp. 2143–2150, 2017.

[33] A. V. Nguyen, L. B. Nguyen, S. Su, and H. T. Nguyen, "Shared control strategies for human-machine interface in an intelligent wheelchair," in *2013 35th Annual International Conference of the IEEE Engineering in Medicine and Biology Society (EMBC)*. IEEE, 2013, pp. 3638–3641.

[34] N. Amirshirzad, A. Kumru, and E. Oztop, "Human adaptation to human–robot shared control," *IEEE Transactions on Human-Machine Systems*, vol. 49, no. 2, pp. 126–136, 2019.

[35] X. Li, G. Chi, S. Vidas, and C. C. Cheah, "Human-guided robotic co-manipulation: two illustrative scenarios," *IEEE Transactions on Control Systems Technology*, vol. 24, no. 5, pp. 1751–1763, 2016.

[36] H. Kiilavuori, V. Sariola, M. J. Peltola, and J. K. Hietanen, "Making eye contact with a robot: Psychophysiological responses to eye contact with a human and with a humanoid robot," *Biological Psychology*, vol. 158, p. 107989, 2021.

[37] T. Onuki, T. Ishinoda, E. Tsuburaya, Y. Miyata, Y. Kobayashi, and Y. Kuno, "Designing robot eyes for communicating gaze," *Interaction Studies*, vol. 14, no. 3, pp. 451–479, 2013.

[38] Y. Song and Y. Luximon, "Trust in AI agent: A systematic review of facial anthropomorphic trustworthiness for social robot design," *Sensors*, vol. 20, no. 18, p. 5087, 2020.

[39] W. K. Juel, F. Haarslev, E. R. Ramírez, E. Marchetti, K. Fischer, D. Shaikh, P. Manoonpong, C. Hauch, L. Bodenhagen, and N. Krüger, "Smooth robot: Design for a novel modular welfare robot," *Journal of Intelligent & Robotic Systems*, vol. 98, no. 1, pp. 19–37, 2020.

[40] B. Porr and F. Wörgötter, "Strongly improved stability and faster convergence of temporal sequence learning by utilising input correlations only," *Neural Computation*, vol. 18, no. 6, pp. 1380–1412, 2006.

[41] R. L. Guimarães, A. S. de Oliveira, J. A. Fabro, T. Becker, and V. A. Brenner, "ROS navigation: Concepts and tutorial," in *Robot Operating System (ROS)*. Springer, 2016, pp. 121–160.

[42] D. Fox, W. Burgard, F. Dellaert, and S. Thrun, "Monte Carlo localization: Efficient position estimation for mobile robots," *AAAI/IAAI*, vol. 1999, no. 343-349, pp. 2–2, 1999.

[43] P. Marin-Plaza, A. Hussein, D. Martin, and A. d. l. Escalera, "Global and local path planning study in a ROS-based research platform for autonomous vehicles," *Journal of Advanced Transportation*, vol. 2018, 2018.

[44] Y. Zhang, Z. Xiao, X. Yuan, S. Li, and S. Liang, "Obstacle avoidance of two-wheeled mobile robot based on DWA algorithm," in *2019 Chinese Automation Congress (CAC)*. IEEE, 2019, pp. 5701–5706.

[45] A. Nasrinahar and J. H. Chuah, "Intelligent motion planning of a mobile robot with dynamic obstacle avoidance," *Journal on Vehicle Routing Algorithms*, vol. 1, no. 2, pp. 89–104, 2018.

[46] J. López, P. Sanchez-Vilariño, M. D. Cacho, and E. L. Guillén, "Obstacle avoidance in dynamic environments based on velocity space optimization," *Robotics and Autonomous Systems*, vol. 131, p. 103569, 2020.

[47] X. Zhou, D. Wang, and P. Krähenbühl, "Objects as points," *CoRR*, vol. abs/1904.07850, 2019. [Online]. Available: http://arxiv.org/abs/1904.07850

[48] F. Schroff, D. Kalenichenko, and J. Philbin, "Facenet: A unified embedding for face recognition and clustering," *CoRR*, vol. abs/1503.03832, 2015. [Online]. Available: http://arxiv.org/abs/1503.03832

[49] N. Farooq, U. Ilyas, M. Adeel, and S. Jabbar, "Ground robot for alive human detection in rescue operations," in *2018 International Conference on Intelligent Informatics and Biomedical Sciences (ICIIBMS)*, vol. 3. IEEE, 2018, pp. 116–123.

[50] S. Coşar and N. Bellotto, "Human re-identification with a robot thermal camera using entropy-based sampling," *Journal of Intelligent & Robotic Systems*, vol. 98, no. 1, pp. 85–102, 2020.

[51] A. Ivanovs, A. Nikitenko, M. Di Castro, T. Torims, A. Masi, and M. Ferre, "Multisensor low-cost system for real time human detection and remote respiration monitoring," in *2019 Third IEEE International Conference on Robotic Computing (IRC)*, 2019, pp. 254–257.

[52] D. Yang, Z. Zhu, J. Zhang, and B. Liang, "The overview of human localization and vital sign signal measurement using handheld IR-UWB through-wall radar," *Sensors*, vol. 21, no. 2, 2021.

[53] S. Steingrube, M. Timme, F. Wörgötter, and P. Manoonpong, "Self-organized adaptation of a simple neural circuit enables complex robot behaviour," *Nature Physics*, vol. 6, no. 3, pp. 224–230, 2010.

[54] J. López-Moliner, C. Vullings, L. Madelain, and R. J. Van Beers, "Prediction and final temporal errors are used for trial-to-trial motor corrections," *Scientific Reports*, vol. 9, no. 1, pp. 1–15, 2019.

[55] J. M. Pearce and G. Hall, "A model for pavlovian learning: variations in the effectiveness of conditioned but not of unconditioned stimuli." *Psychological Review*, vol. 87, no. 6, p. 532, 1980.

[56] R. Shadmehr, M. A. Smith, and J. W. Krakauer, "Error correction, sensory prediction, and adaptation in motor control," *Annual Review of Neuroscience*, vol. 33, pp. 89–108, 2010.

[57] D. J. Herzfeld, P. A. Vaswani, M. K. Marko, and R. Shadmehr, "A memory of errors in sensorimotor learning," *Science*, vol. 345, no. 6202, pp. 1349–1353, 2014.

[58] T. S. Braver, "The variable nature of cognitive control: a dual mechanisms framework," *Trends in Cognitive Sciences*, vol. 16, no. 2, pp. 106–113, 2012.

[59] Q. Yu, B. K. Chau, B. Y. Lam, A. W. Wong, J. Peng, and C. C. Chan, "Neural processes of proactive and reactive controls modulated by motor-skill experiences," *Frontiers in Human Neuroscience*, vol. 13, 2019.

[60] V. Braitenberg, *Vehicles: Experiments in synthetic psychology*. MIT press, 1986.

[61] D. Nakhaeinia, S. H. Tang, S. M. Noor, and O. Motlagh, "A review of control architectures for autonomous navigation of mobile robots," *International Journal of the Physical Sciences*, vol. 6, no. 2, pp. 169–174, 2011.

[62] E. Baklouti, N. B. Amor, and M. Jallouli, "Reactive control architecture for mobile robot autonomous navigation," *Robotics and Autonomous Systems*, vol. 89, pp. 9–14, 2017.

[63] P. Manoonpong and H. Roth, "Reactive neural control for autonomous robots: From simple wheeled robots to complex walking machines," in *Proceedings of the Fifth International Conference on Neural Networks and Artificial Intelligence (ICNNAI'2008)*, 2008.

[64] K. Fischer, J. Seibt, R. Rodogno, M. K. Rasmussen, A. Weiss, L. Bodenhagen, W. K. Juel, and N. Krüger, "Integrative social robotics hands-on," *Interaction Studies*, vol. 21, no. 1, pp. 145–185, 2020.

[65] B. C. Kok and H. Soh, "Trust in robots: Challenges and opportunities," *Current Robotics Reports*, pp. 1–13, 2020.

[66] N. Mitsunaga, C. Smith, T. Kanda, H. Ishiguro, and N. Hagita, "Adapting robot behavior for human–robot interaction," *IEEE Transactions on Robotics*, vol. 24, no. 4, pp. 911–916, 2008.

[67] W. Wang, Y. Chen, R. Li, and Y. Jia, "Learning and comfort in human–robot interaction: A review," *Applied Sciences*, vol. 9, no. 23, p. 5152, 2019.

[68] M. Gupta, S. Kumar, L. Behera, and V. K. Subramanian, "A novel vision-based tracking algorithm for a human-following mobile robot," *IEEE Transactions on Systems, Man, and Cybernetics: Systems*, vol. 47, no. 7, pp. 1415–1427, 2016.

[69] M. Tarokh and R. Shenoy, "Vision-based robotic person following in fast walking," in *2014 IEEE International Conference on Systems, Man, and Cybernetics (SMC)*. IEEE, 2014, pp. 3172–3177.

[70] M. J. Islam, J. Hong, and J. Sattar, "Person-following by autonomous robots: A categorical overview," *The International Journal of Robotics Research*, vol. 38, no. 14, pp. 1581–1618, 2019.

[71] R. Algabri and M.-T. Choi, "Deep-learning-based indoor human following of mobile robot using color feature," *Sensors*, vol. 20, no. 9, p. 2699, 2020.

[72] C. Pang, H. Liu, and X. Li, "Multitask learning of time-frequency cnn for sound source localization," *IEEE Access*, vol. 7, pp. 40 725–40 737, 2019.

[73] F. Haarslev, D. Docherty, S.-D. Suvei, W. K. Juel, L. Bodenhagen, D. Shaikh, N. Krüger, and P. Manoonpong, "Towards crossmodal learning for smooth multimodal attention orientation," in *International Conference on Social Robotics*. Springer, 2018, pp. 318–328.

[74] T. Schulz, P. Holthaus, F. Amirabdollahian, and K. L. Koay, "Humans' perception of a robot moving using a slow in and slow out velocity profile," in *2019 14th ACM/IEEE International Conference on Human-Robot Interaction (HRI)*. IEEE, 2019, pp. 594–595.

[75] F. Graf, Ç. Odabaşi, T. Jacobs, B. Graf, and T. Födisch, "Mobika-low-cost mobile robot for human-robot interaction," in *2019 28th IEEE International Conference on Robot and Human Interactive Communication (RO-MAN)*. IEEE, 2019, pp. 1–6.

[76] M. Skubic, D. Perzanowski, S. Blisard, A. Schultz, W. Adams, M. Bugajska, and D. Brock, "Spatial language for human-robot dialogs," *IEEE Transactions on Systems, Man, and Cybernetics, Part C (Applications and Reviews)*, vol. 34, no. 2, pp. 154–167, 2004.

[77] A. Koller, T. Baumann, and A. Köhn, "Dialogos: Simple and extensible dialogue modeling," in *Proc. Interspeech 2018*, 2018, pp. 167–168.

[78] T. Kuremoto, K. Hashiguchi, K. Morisaki, S. Watanabe, K. Kobayashi, S. Mabu, M. Obayashi *et al.*, "Multiple action sequence learning and automatic generation for a humanoid robot using RNNPB and reinforcement learning," *Journal of Software Engineering and Applications*, vol. 5, no. 12, p. 128, 2013.

[79] L. Patanè, R. Strauss, and P. Arena, "Learning spatio-temporal behavioural sequences," in *Nonlinear Circuits and Systems for Neuro-inspired Robot Control*. Springer, 2018, pp. 65–85.

[80] J. Quintas, G. S. Martins, L. Santos, P. Menezes, and J. Dias, "Toward a context-aware human–robot interaction framework based on cognitive development," *IEEE Transactions on Systems, Man, and Cybernetics: Systems*, vol. 49, no. 1, pp. 227–237, 2019.

Alejandro Pequeño-Zurro was a Research Assistant in the Embodied AI and Neurorobotics Lab at the University of Southern Denmark. His research interests include active sensing, artificial olfaction, sensorimotor coupled systems, and neurorobotics.

Jevgeni Ignasov was a master's degree student in Robot Systems (Advanced Robotics Technology) at the University of Southern Denmark. He holds a bachelor's degree in Mechatronics and has worked in the field of bio-inspired robotics and machine learning.

Eduardo R. Ramírez was a Research Assistant at the SDU Robotics group. He holds a master's degree in Automatic Control and Robotics, and a bachelor's in Mechatronics. For the last two years he has been working on the integration, deployment, and cognition development of welfare mobile robots, both in the private sector as well as academia.

Frederik Haarslev was a Ph.D. fellow at the University of Southern Denmark in the SDU Robotics group. His research interests include deep learning, convolutional neural networks, computer vision, robotics, and human-robot interaction.

William K. Juel received a master's degree in Health and Welfare Technology from the University of Southern Denmark in 2017. He was a Ph.D. fellow in SDU Robotics at the University of Southern Denmark. His research interests include robotics, computer vision, and machine learning.

Leon Bodenhagen holds a Ph.D. degree in Robotics and is an Associate Professor at the University of Southern Denmark. His research interests cover topics related to robotics in the welfare domain such as human-robot interaction, and computer vision and multimodal perception.

Norbert Krüger focuses on research into Cognitive Vision and Robotics, in particular, vision-based manipulation, learning, and welfare robotics. He has published over 60 papers in journals and more than 100 papers at conferences, covering topics such as computer vision, robotics, neuroscience, and cognitive systems.

Danish Shaikh received his Ph.D. degree in BioRobotics from the University of Southern Denmark in 2012. Since 2021 he has been employed as an Associate Professor in Embodied AI and Neurorobotics at the University of Southern Denmark. His research interests include biologically-feasible learning, multi-sensory integration, computational neurorobotics, soft robotic perception, and bio-inspired and biomimetic robotics.

Iñaki Rañó holds an MSc in Physics and a Ph.D. in Computer Sciences from the University of the Basque Country (Spain). He was an Assistant Professor with SDU Biorobotics of the University of Southern Denmark and has held research and teaching positions at the University of Zaragoza (Spain), Ruhr-Universität Bochum (Germany) and Ulster University (UK). He has co-authored over 70 papers on topics such as biorobotics, reinforcement learning, tactile sensing, and decision-making.

Poramate Manoonpong (Senior Member, IEEE) received a Ph.D. degree in Electrical Engineering and Computer Science from the University of Siegen, Germany, in 2006. He is currently a Professor of Biorobotics at the University of Southern Denmark. He has also served as a Professor at the School of Information Science and Technology at Vidyasirimedhi Institute of Science and Technology (VISTEC), Thailand. His research interests include bio-inspired robotics, neural control, embodied cognitive robotics, exoskeleton control, human-machine interaction, exoskeletons, brain-machine interface, and service/inspection robots.